Journal Pre-proof

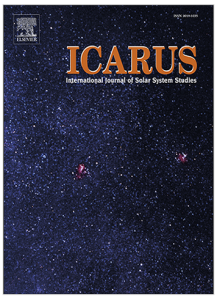

Observations of a dust tail gap in comet C/2014 Q1 (PanSTARRS)

Qasim Afghan, Geraint H. Jones, Oliver Price, Andrew Coates

PII: S0019-1035(22)00378-5
DOI: https://doi.org/10.1016/j.icarus.2022.115286
Reference: YICAR 115286

To appear in: *Icarus*

Received date : 24 May 2022
Revised date : 18 September 2022
Accepted date : 19 September 2022

Please cite this article as: Q. Afghan, G.H. Jones, O. Price et al., Observations of a dust tail gap in comet C/2014 Q1 (PanSTARRS). *Icarus* (2022), doi: https://doi.org/10.1016/j.icarus.2022.115286.

- A new dust tail structure, a dust tail gap, has been observed in comet C/2014 Q1.
- This presents as a single large section of the dust tail devoid of dust.
- The gap's structure was analysed using the Finson-Probstein model.
- This has been spotted in 3 other comets, and all these gaps form around perihelion.
- Potential formation processes for this new feature are discussed.

Observations of a Dust Tail Gap in Comet C/2014 Q1 (PanSTARRS)

Qasim Afghan,[1,2] Geraint H. Jones,[1,2] Oliver Price,[1,2] and Andrew Coates[1,2]

[1] *Mullard Space Science Laboratory, University College London, Holmbury St. Mary, Dorking, Surrey RH5 6NT, UK*
[2] *The Centre for Planetary Sciences at UCL/Birkbeck, London, UK*

ABSTRACT

Cometary dust tails display a wide array of structures, most believed to be caused by a variable dust production, size distributions, fragmentation processes, and interactions with the solar wind, e.g. Price et al. (2019). However, not all these structures are fully understood. Here we report the discovery of a curious new dust tail feature, first noted in long period comet C/2014 Q1 (PanSTARRS) (Bolin et al. 2014), where a section of the dust tail was clearly missing. This implies that the comet underwent a dramatic temporary decrease in dust production near perihelion. The gap appeared on 2015 July 14, 8 days after perihelion at 0.318 au, and progressed along the tail, following the expected motion of the dust that should have been present. The gap corresponds to dust ejected between July 5 and July 12, and of β >0.01. Possible explanations for this gap are proposed.

Keywords: comets

1. INTRODUCTION

C/2014 Q1 displayed an atypical cometary brightness profile, experiencing a period of rapid and significant brightening a few days before perihelion (Combi et al. 2018). Its perihelion on 2015 July 6 was at a distance of 0.318 au. The images analysed here were all taken post-perihelion, from July 14 to the end of August, after which the observing geometry was poor. As no professional images are available, all data used here are solely from amateur astronomers. These are a highly valuable resource, but there are important caveats to using amateur images from various sources, such as the common use of post-processing techniques that distort the original, true image. All the data in this report have been carefully collected and contain none of these adjustments.

On July 16 (Figure 1 (a)), there were no obvious gaps in the dust tail, only a seemingly typical separation between the dust tail and the predominantly blue ion tail. However, as time passed and more dust was ejected, the 'gap' between the bulk of the dust tail and the ion tail continued to expand and newly ejected dust was visible in the ion tail area. This gap became progressively more obvious, becoming very clear by late July (Figure 1 (b)). The 'gap' remained present in all the later images. Observers at the time understandably assumed that the gap was the separation of a typical Type II dust tail and Type III dust *trail* close to or along the comet's orbit, e.g. Sykes & Walker (1992), so the gap's true nature went unnoticed.

2. METHOD

The astrometric data for the amateur images used was attained using the online software astrometry.org (Lang et al. 2010). Efforts were made to parameterise the gap using a simplified Finson-Probstein model (Finson & Probstein 1968). The model simulates the trajectorie s of dust particles ejected by the comet, which are dependent on the ratio of the solar radiation pressure and the gravitational force exerted by the Sun on the dust particles, usually denoted by β (e.g. Fulle (2004)). This β parameter is, very broadly, inversely related to the size of the dust grains (Burns et al. 1979). The dust tail of C/2014 Q1 was simulated using the Finson-Probstein model and was overlaid onto the image, e.g. Figure 2. The properties of the dust particles that 'should' have been present in the gap could then be ascertained, namely their β values and the time at which they were ejected. The temporal plots used in 3.2 are a novel analysis technique developed by Oliver Price (Price et al. 2019). The overlaid simulated tails in the Finson-Probstein plots enable β and ejection time values to be attributed to each pixel in the image. As a result, the image can then be transformed and plotted in a β vs ejection-time parameter space.

3. RESULTS

3.1. *Finson-Probstein Model Analysis*

Date and Time of Image	Observer	Heliocentric Distance (AU)
2015/07/16 17:10	Michael Jäger	0.436
2015/07/17 17:30	Michael Jäger	0.457
2015/07/18 17:20	Michael Jäger	0.477
2015/07/21 17:27	Michael Jäger	0.539
2015/07/22 06:45	Ian Griffin	0.552
2015/08/03 07:29	Minoru Yoneto	0.811
2015/08/10 18:00	Rooisand Observatory	0.965
2015/08/11 09:00	José J. Chambó	0.978
2015/08/13 08:45	José J. Chambó	1.018
2015/08/14 08:44	Damian Peach	1.038
2015/08/17 08:42	Damian Peach	1.097
2015/08/18 08:55	Damian Peach	1.117
2015/08/19 08:58	Damian Peach	1.136
2015/08/22 09:03	Damian Peach	1.194

Table 1. A list of the images used to produce the data displayed.

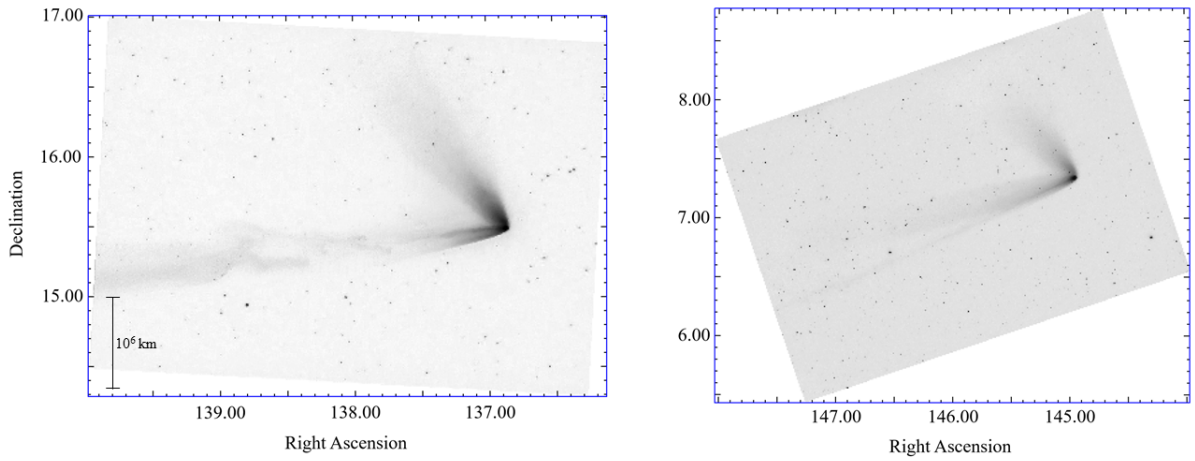

Figure 1. Images of C/2014 Q1 (PanSTARRS), both taken by Michael Jäger. Left to right: (a) 2015 July 16 17:25; (b) greyscale image, 2015 July 21 17:27 (all times UTC). All images are aligned with North upwards, and are plotted on Right Ascension and Declination axes (units in degrees). A scale bar of $10^6 km$ is provided in the bottom left hand corner of (a), but applies to both images. The broad ion tail, one section of the dust tail and a gap between them are visible in (a), but without the second section of dust visible in this image its difficult to identify the dust tail gap. By (b), the dust tail is clearly split into two large segments, separated by a wedge shaped gap. The ion tail in (b) is still visible but much fainter, presenting itself as a long, much thinner streak pointing South West. The dust trail is not visible in these images, but is expected to be a thin line pointing in the North East direction.

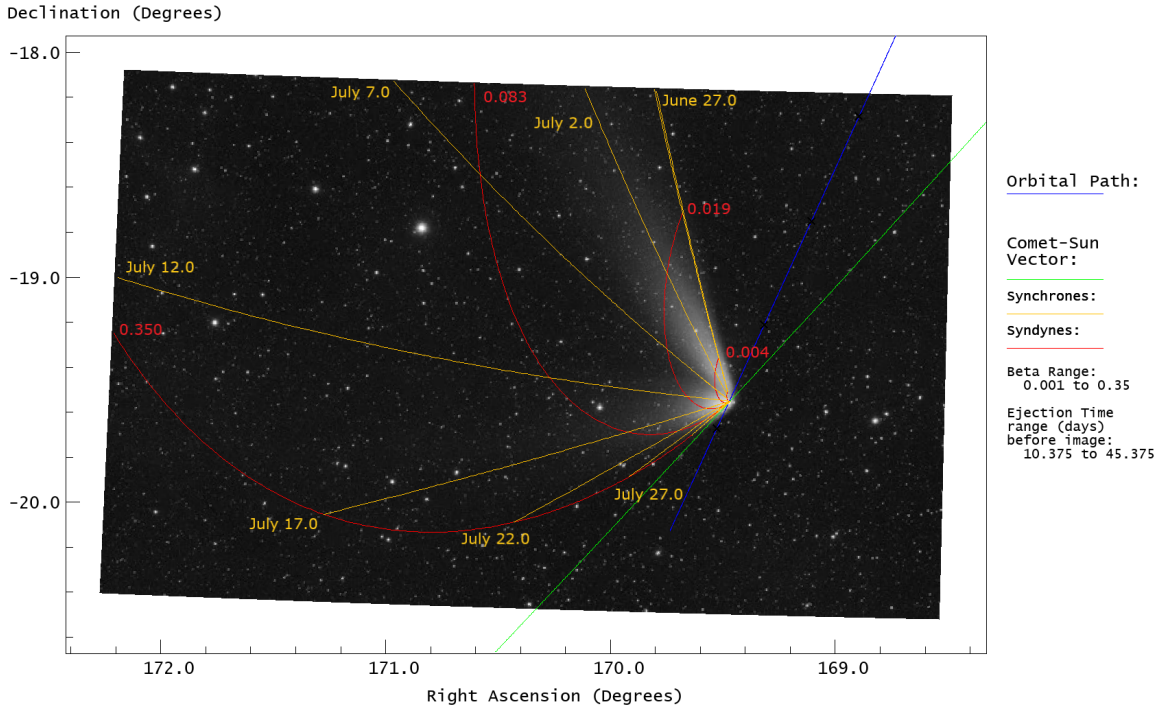

Figure 2. A Finson-Probstein modelled dust tail overlaid onto an image taken on 2015 August 11 09:00 UTC. The blue line shows the comet's orbital path, and green line the comet-Sun vector, which is the direction of radiation pressure on the dust grains. The red lines denote syndynes, which are lines of constant dust β. The yellow lines denote synchrones: lines of constant dust age, labelled with the date of the respective dust ejection. Only 7 synchrones are included in this plot for clarity. The July 7.0 and July 12.0 synchrones align well with the tail gap's boundaries.

Finson-Probstein analysis for several images (see Figure 2 and Methods section) showed that the dust tail gap was consistently bounded by synchrones for dust ejected at approximately July 5 (heliocentric distance, $r_H = 0.318$ AU) and July 12 ($r_H = 0.355$ AU). General boundary conditions for the entire dust tail indicate the initiation of significant dust emission around June 22 ($r_H = 0.525$ AU). The β range of the comet's visible dust tail is observed to be $\lessapprox 0.2$. Using the rough approximation that dust grain size, in microns, is equal to the reciprocal of β, suggests a minimum grain size of ~5µm (Burns et al. 1979). This assumes a particle density of $\rho_d = 0.5$ g cm^{-3} and a scattering efficiency for radiation pressure of $Q_{pr} = 1$.

3.2. *Temporal Plots*

To investigate this further, images were transformed and plotted in dust β – ejection time parameter space (Figure 3), referred to hereon as temporal plots, as first presented by Price et al. (2019). One of the images analysed was taken on August 11 (Figure 2). For direct comparison, the x-axis (Date of Ejection) was fixed to always display dust ejected between June 22 and July 16 ($r_H = 0.423$ AU). The clarity of the gap changed due to different image qualities and exposure times, however the gap's "ejection time" range was consistently bounded by the July 5 and 12 synchrones, confirming it as a physical feature. The gap is clear and present at approximately $\beta > 0.01$, but below this value there *appeared* to be a significant amount of dust present as seen in Figure 3, but this overlapped with the comet's coma. At $\beta > 0.05$ the gap appears very dark, suggesting it was almost completely devoid of dust. However at approximately $0.05 > \beta > 0.01$, there appeared to still be some dust present. Dust-sparse areas are particularly obvious near the gap's boundaries in the temporal plots, corresponding to dust ejected just after July 5 and shortly before July 12. Furthermore, some images showed the gap did extend to $\beta < 0.01$ as a translucent, less populated tail region. This

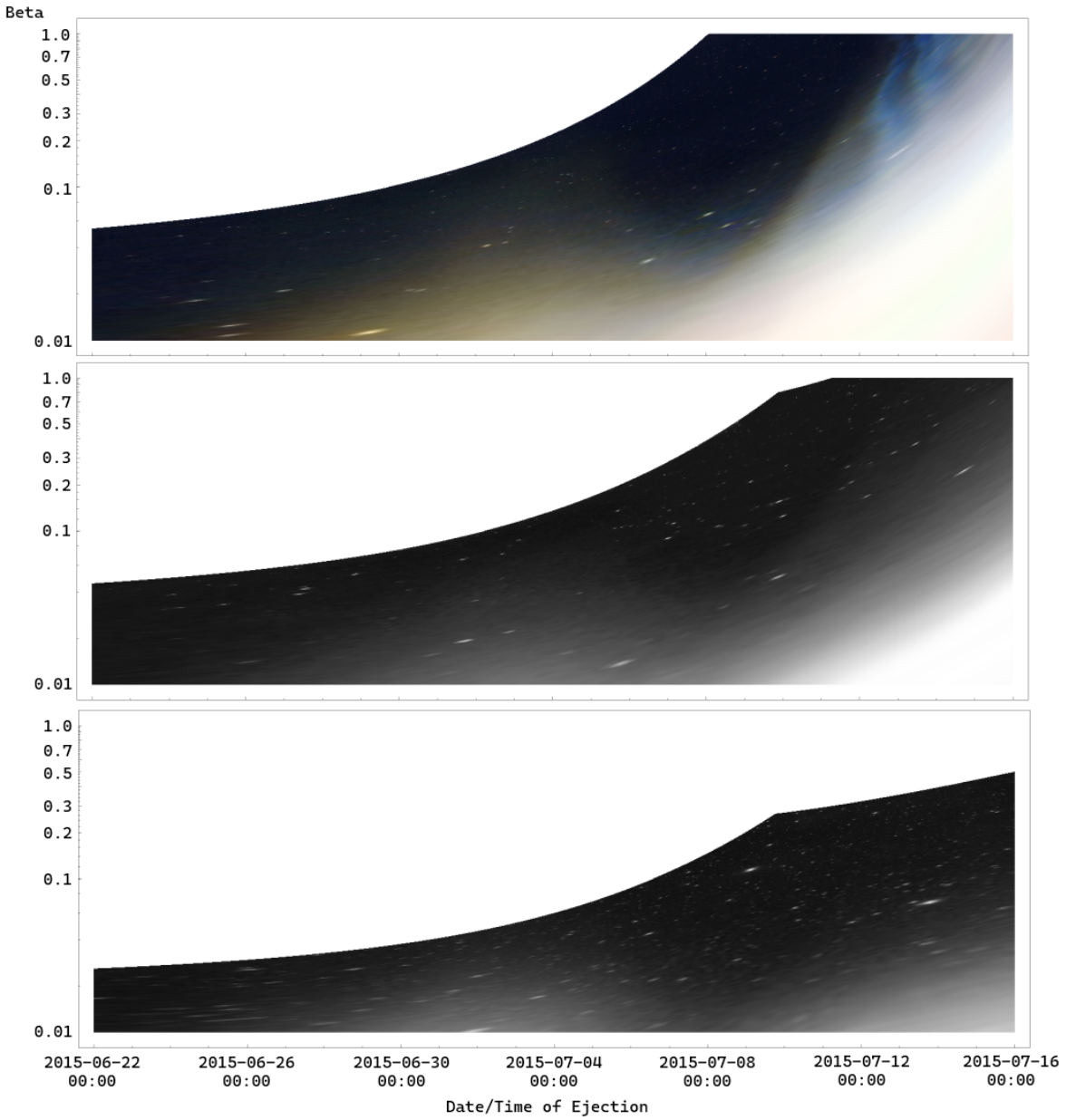

Figure 3. Temporal plots of the images taken on July 18, July 21 (Figure 1(b)) and August 11, from top to bottom. Dust β is on the y-axis as a logarithmic axis, with the bottom of each image corresponding to a minimum beta value of 0.01. Date and time of dust ejection is on the x-axis. The dust gap can be seen between July 5 and July 12, with the gap darker at higher β values.The plots share the same x-axis, demonstrating that over time the gap does not shift in β-ejection time parameter space.The apparent size of the gap is reduced in the temporal plots due to the logarithmic y-axis, leading to an over-representation of the $\beta < 0.1$ region.

gap extension lay outside the July 5 – 12 range discussed above, extending to July 3 ($r_H = 0.332AU$), and was not present in all images.

3.3. *Statistical Analysis*

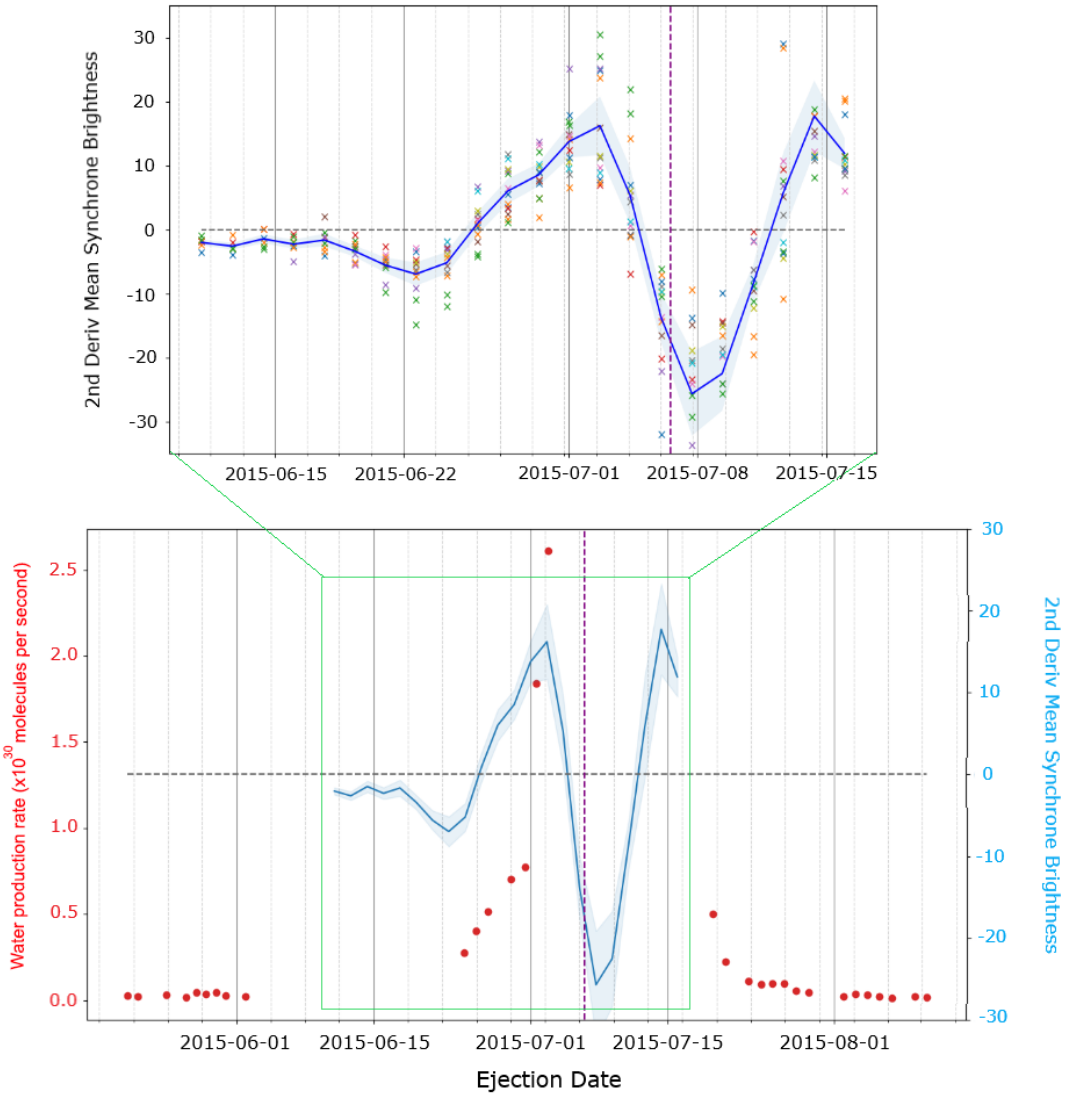

Figure 4. Top: date of dust ejection (x-axis) vs. the second derivative of mean synchrone pixel brightness (y-axis). Each plot colour is attributed with an image of the comet. The blue line represents the mean of all the images considered, with the blue shaded area demonstrating a confidence level of 95%. There is a clear dip in the graph between July 5 and July 12. Bottom: a comparison of the water production rate of C/2014 Q1 from the SOHO SWAN instrument (red, y-axis on the left hand side) to the mean synchrone brightness trendline (blue, y-axis on the right hand side). Date of dust ejection is on the x-axis, and a dotted grey line has been plotted to signify the zero-point for the mean synchrone brightness. The shaded blue region shows the 95% confidence level in the mean synchrone brightness trendline. For both plots, the vertical purple dashed line shows the comet's perihelion date on 2015 July 6.

The average brightness of each synchrone (corresponding to columns of pixels in Figure 3) was plotted for all images. Variations in the amateurs' image parameters meant that an absolute comparison would be ineffective. Furthermore, the dust tail dims with increasing distance from the nucleus, with a resultant decrease in signal to noise ratio. This causes the gap to be less identifiable in the plot. To account for this, the second derivative of the average synchrone brightness graph was calculated (Figure 4). This would accentuate any dips in the average synchrone brightness, revealing any underlying patterns that were otherwise obscured by the general trend of decreasing brightness with dust age. The 'gap' in the tail should appear as a section where the second derivative of the average brightness dips below zero: an area within which the brightness of the tail is decreasing more rapidly than the underlying brightness reduction of the tail as it extends away from the nucleus. As shown, the main dip in the graph lies between approximately July 5 and 12 for all images considered, agreeing with the visual inspection results.

3.4. *Dust Gap Structure*

The tail gap's edges are curved in relation to the synchrones. In the temporal plots (Figure 3), structures associated with dust ejection time or dust β would appear in columns or rows respectively, yet the gap is also curved in these plots and does not precisely follow lines of constant dust ejection time nor β. Some of the images also show that the end of the dust tail gap, around July 12, was not a well-defined step up in activity. July 21 and 22 images show that the dust tail region around the July 12 synchrone was significantly dimmer than the dust released from approximately July 14 onwards ($r_H = 0.387AU$). There is a visible boundary between the sparser dust region centred around the July 12 synchrone and the denser dust region released after that. This gradual 'restart' of dust production can be seen in the temporal plots: the gap is darkest in the middle, but brighter nearer its edges. Discrete increases in dust tail brightness visible in July 21 and 22 images most likely confirm that this is physical. These structures could provide insight into what caused this tail gap, but also highlights the difficulties in defining boundaries for this gap.

3.5. *Water Production Rate*

The comet's water production rate was measured from SOHO spacecraft SWAN data between 2015 May 20 and August 10 (Combi et al. 2018). C/2014 Q1 had a unique and unusual activity profile around perihelion. Approaching perihelion, its water production increased by a factor of ∼100 over ∼20 days, and dropped by a similar factor post-perihelion. The comet is inferred to have lost approximately 64% of its mass during this period, signifying a potential fragmentation event. A comparison of the water production rate and the second derivative of the synchrone brightness can be seen in Figure 4. We see a strong correlation between June 22 and July 2 ($r_H = 0.343AU$), where both datasets display a clear increase in activity. This also correlates with the visual analysis of Figure 2, where it is clear that the dust tail is observable from the June 22 synchrone onwards, as discussed in 3.1. Lastly, the visual magnitude data shows a brief spike in brightness during perihelion that is a magnitude larger than the modelled brightness profile (Yoshida 2022). This large increase in brightness starts on July 5th and runs until July 7th, coinciding with the start of the dust tail gap. There is no visual data available until July 12th, coinciding with the end of the gap, by which time the magnitude has dropped back to expected levels during perihelion.

Unfortunately, there are also significant gaps in the SWAN water production rate data, when the comet was near solar conjunction, including July 3-16, during which the tail gap formed. Visual interpolation of the water production rate shown in Figure 4 suggests that this dust tail gap appears right at the highest measured water production level. Water production then fell dramatically by July 18 ($r_H = 0.462AU$); a large increase in the mean synchrone brightness around July 12 signified the end of the dust tail gap, but the small decrease in brightness on July 15 tracks the falling water production rate data.

This provides some validation for our results, which is useful when using unregulated amateur images. Information on the activity and structure of the comet nucleus is of great value when investigating dust tail structure. This unusual activity also roughly coincides with the formation of the dust tail gap. The connection between the two events is discussed in detail in 4.2.

3.6. *Possible Dust Tail Gaps in Other Comets*

Three other comets are reported here to display a similar gap in their dust tails: C/2002 F1 (Utsunomiya), C/2000 WM1 (LINEAR) and the Great January Comet of 1910, C/1910 A1 (Figure 5). Whilst these dust tails have been analysed, the image datasets for these comets are severely limited both in quality and quantity. Consequently, these comets are noteworthy but high-confidence results are unavailable.

C/2002 F1 displayed a gap most similar to that of C/2014 Q1. Its gap was bounded by synchrones corresponding to ejection 4 days before and 2 days after the comet's perihelion on 2002 April 22. The comet's light curve displayed a significant brightness dip at perihelion (Filonenko & Churyumov 2004). The start and end of this dip accurately match the synchrone dates that bound the observed dust tail gap. Furthermore, the timing of this dust tail gap accurately matches a V-shaped dip in the visual magnitude readings for the comet, which was unavailable for C/2014 Q1. Unfortunately, only three high-quality images were available to analyse, spanning April 30 - May 1.

The gap in the dust tail of C/2000 WM1 is much narrower and less clear than the gaps in the comets discussed thus far. This is mainly due to the viewing geometry of the dust tail from Earth. However, analysis of the available images shows that this gap is also bounded by synchrones corresponding to dust that should have been ejected six days and eight days after the comet's perihelion on 2002 January 22. Whilst this gap appears around perihelion, it does not coincide with a dip in the light curve of the comet (Filonenko & Churyumov 2004).

The lack of data hinders any in-depth analysis for these comets at this point, however initial analysis shows that these are promising candidates of dust tail gaps and is further supporting evidence that the dust tail gap of C/2014 Q1 is physical.

Comet	Perihelion Date	Perihelion Distance (AU)	Dust Tail Gap Period (days)
C/2014 Q1 (PanSTARRS)	2015/07/06.5	0.315	$p-1 >> p+6$
C/2002 F1 (Utsunomiya)	2002/04/22.9	0.438	$p-4 >> p+2$
C/2000 WM1 (LINEAR)	2002/01/22.7	0.555	$p+6 >> p+9$
C/1910 A1	1910/01/17.6	0.129	$p-1 >> p+2$

Table 2. A summary of the key features of all the comets with dust tail gaps currently observed. The comets are arranged in chronological order. In the Dust Tail Gap Period column, 'p' refers to the date of perihelion. For example, the first value in this column indicates a dust tail gap that starts one day before perihelion ('p-1') and ends six days after perihelion ('p+6').

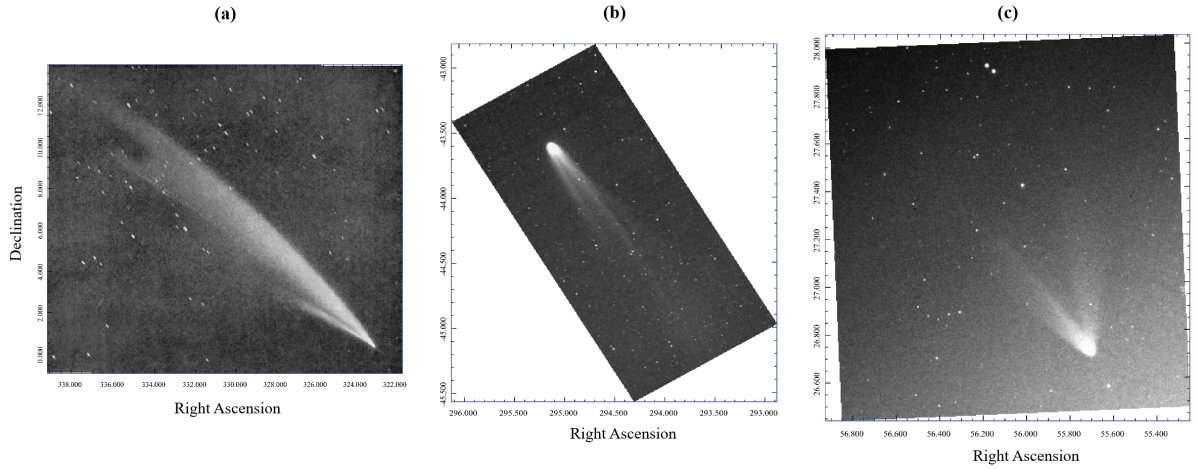

Figure 5. Images of three other comets with potential dust tail gaps. From left to right: (a) C/1910 A1 on 1910 January 29; (b) C/2000 WM1 (LINEAR) on 2002 February 3; (c) C/2002 F1 (Utsunomiya) on 2002 April 30 . Each comet had two distinct sections in its dust tail, with a gap in between them. For all three comets, the sections have been confirmed to be part of the dust tail, and not a typical separation between dust tail and trail. Images taken, from left to right, by: Stockholm Observatory, Manawatu Observatory, Michael Jäger.

4. DISCUSSION

Some potential causes of the gap can be dismissed. Although close to the heliocentric distance needed to be classified as a near-Sun comet (Jones et al. 2017), solar insolation was insufficient for dust grain destruction. Furthermore, dust grains elsewhere in the tail, ejected at a similar heliocentric distance, were still visible. The possibility of a coronal mass ejection or other solar event causing this dust gap is also considered very unlikely. No realistic solar-related scenario can be envisioned for this discrete gap, and no large solar events directed at the comet were documented around the time of perihelion. We describe more promising potential causes in more detail below.

4.1. *Comet Activity Fluctuation*

The apparently well-defined dust gap ejection time suggests that between July 5 and 12, the dust output of the comet was reduced. Maybe this was a seasonal effect, i.e. that exposed volatile ices were only present on one side of the comet. As a result, less ice sublimated during this period and so much less dust was shed. Periods of reduced sublimation have been observed on areas of the nucleus of 67P/Churyumov-Gerasimenko, although only surface-level activity was tracked and its exact effects on the dust tail were not observed. One of the few similarities between the comets presented here are that none of them are dynamically new, based on the reciprocal of their original semi-major axis values (in AU) retrieved from the Minor Planet Center Database, with the exception of C/2002 F1 (Utsunomiya) which had an undetermined value(Oort & Schmidt 1951). Thus, these comets could have highly evolved surfaces due to their several transits through the inner Solar System. This might result in areas devoid of volatile ices.

However, synchronic bands are periodic features: in the case of C/2014 Q1, there is only one dust gap. Over the two months of observations following the formation of this gap, there were no other gaps observed. Most of the rotational periods of comets measured are on the order of a few hours to a couple of days (Kokotanekova et al. 2017). It can thus be concluded that this gap is not a periodic feature. However seasonal effects, as well as the complex rotational dynamics of comet nuclei, can affect dust activity on longer timescales, as discussed below in 4.2 (A'Hearn et al. 2011).

Nucleus surface conditions could also play an important role. Rosetta mission results showed local surface properties limiting dust production during peak water production periods, in particular the cohesion strength between dust grains and the porosity of the surface dust layer (Tubiana et al. 2019). In the case of C/2014 Q1, this explanation suffers the same shortcomings mentioned above, as this area would be insolated periodically due to the comet's rotation and thus this gap would reoccur. However, the similarity in water and dust production rates makes this study relevant to this investigation. Alternatively, there could be a region on the nucleus that has a layer of fallback material primarily consisting of larger dust grains or icy grains. If this region was in winter for most of the orbit, the gas flux in this region would be low during that time, allowing the smaller grains to reach escape velocity but causing all the larger grains to fallback onto the nucleus. This scenario has been seen during the Rosetta mission at 67P (Thomas et al. 2015). This would explain why the gap is not present at smaller β values, although whether this is physical or due to gas contamination of the images is still undetermined.

The presence of large dust grains and lack of smaller grains was also observed at 2P/Encke, which was correlated with a reduced gas flux at the time (Rosenbush et al. 2020). However, the lack of activity data during the period of the tail gap for C/2014 Q1 hinders any comparison between these two events, and evidence for an outburst immediately before the start of the tail gap period would make this explanation less likely.

4.2. *Icy Grains in the Dust Tail*

Ice grains have been extensively observed in other comets and their dust tails (Hanner 1981; Protopapa et al. 2018; Sunshine & Feaga 2021). These icy grains ranged from ∼µm to ∼cm in size (Sunshine et al. 2007; A'Hearn et al. 2011). These grains sublimate, accelerating them in the anti-sunward direction whilst decreasing in size. When C/2014 Q1 was around perihelion, at heliocentric distances of is ∼0.3 – 0.4 au, the lifetime of small and impure ice grains was very short - a few minutes or hours.

There could have been a period where almost all ejected particulates were ice-dominated, as seen in other comets' outbursts (Kelley et al. 2020). It could be concluded that the peak seen in water production naturally corresponds to a peak in ice grain ejection, so at the height of water production the ejected dust would have been ice-dominated and hence short-lived, leading to this dust tail gap. The start of the dust tail gap also coincides with an outburst seen in the visual magnitude data, as discussed in 3.5. However, if sublimating ice grains were the cause, many more of these gaps would have already been observed at other comets. Furthermore, the fact that the gap edges align accurately with the synchrones is not well explained by this scenario.

Both the activity fluctuation and the ice-grain sublimation explanations rely on an area of the comet nucleus with special properties (either ice-dominated or ice-sparse) constantly facing the Sun for 7 days during perihelion. This

would occur if C/2014 Q1 had a high obliquity. If during perihelion, the rotational axis was roughly aligned with the Sun-comet radial vector, only one side of the nucleus would be insolated during this period. This alignment would not be periodic during a single orbital transit, satisfying the conditions required to produce the tail feature seen. These conditions are unlikely but have been observed before (e.g. at 2P/Encke (Rosenbush et al. 2020) (Sekanina 1988)), which is fitting for a tail feature that is rarely seen. Thus, it would be at these high latitudes on the nucleus, where these ice-dense or ice-sparse regions would lie. These regions could remain in winter for much of the comets orbit pre-perihelion, thus preserving their state until insolation around perihelion.

4.3. *Optical Depth Effects*

Considering the high activity of C/2014 Q1 around perihelion, the increased inner coma optical depth could have played a major role. An optical depth increase would reduce the amount of solar radiation reaching the nucleus, instead being scattered by coma particles. If this reduction were significant enough, the rate of ice sublimation on the nucleus could reduce to the point where the amount of dust produced by the comet was minimal (e.g. Hellmich & Keller (1980)).

Similarly, the increase in scattering of solar radiation could reduce the acceleration of dust particles out of the coma and into the dust tail: there would be a more isotropic radiation pressure as opposed to the usual anti-solar directional pressure (Müller et al. 2002). Consequently, the dust particles would enter the dust tail at a much lower rate. Dust ejected during this period could be concentrated in the low-β region of the dust tail, as the reduced radiation pressure results in a reduced effective β for these particles. Once the optical depth of the coma reduces, these particles could then have a delayed acceleration and experience the usual grain size-dependent separation. The model developed in Müller et al. (2002) calculates that ambient radiation surpasses solar radiation at the nucleus when the optical depth increases above an approximate value of $\tau = 5$. This is a significant increase in optical depth, and the likeliness of this scenario is uncertain.

Highly active comets in the recent past haven't displayed a dust tail gap, such as C/1995 O1 (Hale-Bopp) and C/2006 P1 (McNaught), though C/2014 Q1 is believed to have a much smaller nucleus radius, of 0.7-1.1 km (Combi et al. 2018). A smaller nucleus, with similar levels of activity to Hale-Bopp and McNaught, could result in a denser coma, and thus larger optical depth.

5. CONCLUSIONS

The existence of the dust tail gap has been verified, adding another unique structural element in cometary dust tails to look out for in future observations. Structure within the gap is also visible, where the dust number density is lowest in the middle of the gap but increasing away from its centre. None of the explanations provided in this study are conclusive, due to the lack of data. The limitations of the C/2014 Q1 dataset mean that any further clarification on the formation of this dust tail gap would be difficult. This gap is rare but, as also reported here, not unprecedented. To further our understanding of dust tail gaps, more examples of this feature need to be observed to add to the dataset. To confirm a dust tail gap requires modelling, but potential candidates can be identified visually. Any potential dust tail gap candidate must ideally show a dust tail split into two distinct and large sections, with a large gap between them. Figure 1(c) and Figure 5(b), as well as any other publicly available image of C/2014 Q1 and C/2002 F1, can be used as reference figures when trying to identify dust tail gaps in other comets. Any cometary dust tails that match this description can be relayed via email to any of the authors of this paper for in-depth analysis.

6. ACKNOWLEDGMENTS

The authors thank the two referees for their valuable feedback and suggestions. QA and OP acknowledge the support of UK Science and Technology Facilities Council (STFC) PhD studentships. GHJ and AJC are grateful to STFC for partial support through consolidated grant ST/S000240/1. We appreciate the contribution of images by: Michael Jäger, José J. Chambó, Lowell Observatory, Manawatu Observatory, Rooisand Observatory, Team Chameleion, Franz Hofmann and Wolfgang Paech. This research has made use of data and/or services provided by the International Astronomical Union's Minor Planet Center.

REFERENCES

A'Hearn, M. F., Belton, M. J. S., Delamere, W. A., et al. 2011, Science, 332, 1396, doi: 10.1126/science.1204054

Bolin, B., Micheli, M., Sato, H., Buzzi, L., & Holmes, R. 2014, Central Bureau Electronic Telegrams, 3933, 1

Burns, J. A., Lamy, P. L., & Soter, S. 1979, Icarus, 40, 1, doi: https://doi.org/10.1016/0019-1035(79)90050-2

Combi, M., Mäkinen, T., Bertaux, J.-L., et al. 2018, Icarus, 300, 33, doi: https://doi.org/10.1016/j.icarus.2017.08.035

Filonenko, V. S., & Churyumov, K. I. 2004, Astronomical School's Report, 5, 115, doi: 10.18372/2411-6602.05.1115

Finson, M. J., & Probstein, R. F. 1968, ApJ, 154, 327, doi: 10.1086/149761

Fulle, M. 2004, Motion of cometary dust, ed. M. C. Festou, H. U. Keller, & H. A. Weaver, 565

Hanner, M. S. 1981, Icarus, 47, 342, doi: https://doi.org/10.1016/0019-1035(81)90182-2

Hellmich, R., & Keller, H. U. 1980, in Solid Particles in the Solar System, ed. I. Halliday & B. A. McIntosh, Vol. 90, 255–258

Jones, G., Knight, M., Battams, K., et al. 2017, Space Science Reviews, 214, doi: 10.1007/s11214-017-0446-5

Kelley, M., Protopapa, S., Moulane, Y., et al. 2020, in AAS/Division for Planetary Sciences Meeting Abstracts, Vol. 52, AAS/Division for Planetary Sciences Meeting Abstracts, 108.01

Kokotanekova, R., Snodgrass, C., Lacerda, P., et al. 2017, MNRAS, 471, 2974, doi: 10.1093/mnras/stx1716

Lang, D., Hogg, D. W., Mierle, K., Blanton, M., & Roweis, S. 2010, AJ, 139, 1782, doi: 10.1088/0004-6256/139/5/1782

Müller, M., Green, S. F., & McBride, N. 2002, Earth Moon Planet., 90, 99, doi: 10.1023/A:1021568502723

Oort, J. H., & Schmidt, M. 1951, BAN, 11, 259

Price, O., Jones, G. H., Morrill, J., et al. 2019, Icarus, 319, 540, doi: https://doi.org/10.1016/j.icarus.2018.09.013

Protopapa, S., Kelley, M. S. P., Yang, B., et al. 2018, ApJL, 862, L16, doi: 10.3847/2041-8213/aad33b

Rosenbush, V., Ivanova, O., Kleshchonok, V., et al. 2020, Icarus, 348, 113767, doi: 10.1016/j.icarus.2020.113767

Sekanina, Z. 1988, AJ, 95, 911, doi: 10.1086/114689

Sunshine, J. M., & Feaga, L. M. 2021, Planetary Science Journal, 2, 92, doi: 10.3847/PSJ/abf11f

Sunshine, J. M., Groussin, O., Schultz, P. H., et al. 2007, Icarus, 190, 284, doi: https://doi.org/10.1016/j.icarus.2007.04.024

Sykes, M. V., & Walker, R. G. 1992, Icarus, 95, 180, doi: https://doi.org/10.1016/0019-1035(92)90037-8

Thomas, N., Sierks, H., Barbieri, C., et al. 2015, Science, 347, aaa0440, doi: 10.1126/science.aaa0440

Tubiana, C., Rinaldi, G., Güttler, C., et al. 2019, A&A, 630, A23, doi: 10.1051/0004-6361/201834869

Yoshida, S. 2022, Seiichi Yoshida. aerith.net